

Controlled rate thermal analysis of sepiolite

Ray L. Frost · János Kristóf · Erzsébet Horváth

Received: 27 October 2008 / Accepted: 3 February 2009 / Published online: 1 September 2009
© Akadémiai Kiadó, Budapest, Hungary 2009

Abstract CRTA technology offers better resolution and a more detailed interpretation of the decomposition processes of a clay mineral such as sepiolite via approaching equilibrium conditions of decomposition through the elimination of the slow transfer of heat to the sample as a controlling parameter on the process of decomposition. Constant-rate decomposition processes of non-isothermal nature reveal changes in the sepiolite as the sepiolite is converted to an anhydride. In the dynamic experiment two dehydration steps are observed over the ~20–170 and 170–350 °C temperature range. In the dynamic experiment three dehydroxylation steps are observed over the temperature ranges 201–337, 337–638 and 638–982 °C. The CRTA technology enables the separation of the thermal decomposition steps.

Keywords Attapulgitite · Sepiolite · Palygorskites · Thermal analysis · CRTA · Thermogravimetry

Introduction

The thermoanalytical studies of palygorskites are not new, even though the first reported studies were in 1947 [1–5]. A lack of recent studies is true of minerals such as palygorskite [6–9]. There is a need to undertake a systematic study using the latest technology of these minerals using thermo-analytical techniques including dynamic and controlled rate thermal analysis. Very few thermo-analytical and spectroscopic studies of the palygorskite have been forthcoming and what studies that are available are not new. To the best of the authors knowledge no recent thermo-analytical studies of sepiolites have been undertaken, especially in recent times, although differential thermal analysis of some related minerals has been published [10, 11]. The objective of this research is the study of the thermal decomposition of two selected sepiolites.

Sepiolites, attapulgitites and various forms of ‘Rocky mountain leather’ all have a fibrous like morphology with a distinctive layered appearance [12–15]. Palygorskite has the structural formula $[(\text{OH}_2)_4(\text{Mg}, \text{Al}, \text{Fe})_5(\text{OH}) \cdot 2\text{Si}_8\text{O}_{20}] \cdot 4\text{H}_2\text{O}$ and sepiolite the formula $[(\text{OH}_2\text{Mg}_8(\text{OH}) \cdot 4\text{Si}_{12}\text{O}_{30}) \cdot 8\text{H}_2\text{O}$. The formulas are written as such to indicate the two types of water present, magnesium coordinated water and adsorbed water. The principal difference between the formula of sepiolite and palygorskite rests with the formula. Sepiolite $[\text{Mg}_8\text{Si}_{12}\text{O}_{30} (\text{OH})_4 \cdot (\text{H}_2\text{O})_4 \cdot 8\text{H}_2\text{O}]$ is a trioctahedral type mineral with three divalent magnesium cations filling the three positions of the octahedron. On the other hand palygorskite with the formula $[(\text{OH}_2)_4(\text{Mg}, \text{Al}, \text{Fe})_5(\text{OH}) \cdot 2\text{Si}_8\text{O}_{20}] \cdot 4\text{H}_2\text{O}$ has some of the magnesium cations replaced with trivalent cations such as Al or Fe, thus palygorskites tend towards a dioctahedral structure.

The dehydration and dehydroxylation of the palygorskite clays have been studied in detail by thermogravimetric

R. L. Frost (✉)
Inorganic Materials Research Program, School of Physical and Chemical Sciences, Queensland University of Technology,
2 George Street, G.P.O. Box 2434, Brisbane, QLD 4001,
Australia
e-mail: r.frost@qut.edu.au

J. Kristóf
Department of Analytical Chemistry, University of Pannonia,
P.O. Box 158, 8201 Veszprém, Hungary

E. Horváth
Department of Environmental Engineering and Chemical
Technology, University of Pannonia, P.O. Box 158, 8201
Veszprém, Hungary

techniques [4, 16, 17]. Differential Thermal Analysis (DTA) in combination with other techniques such as X-ray diffraction and Fourier Transform infrared spectroscopy (FTIR) proved most useful for the study of the dehydration process. It was found that dehydration of sepiolite and attapulgite take place in a series of four steps [18–20]. Up to 200 °C both hygroscopic and zeolitic water were lost. Between 250 and 450 °C bound water was lost; more strongly bound water was lost in the temperature range 450–610 °C; and coordinated water was lost in the temperature range 730–860 °C. All of the dehydration steps were endothermic in DTA. For both minerals, the partial dehydration of bound H₂O in the ranges 250–610 °C and 210–550 °C resulted in the formation of sepiolite anhydride and palygorskite anhydride, respectively. Dehydration of the bound H₂O in two steps was attributed to the difference in bonding position of H₂O in the structure of these minerals.

Thermal analysis using thermogravimetric techniques enables the mass loss steps, the temperature of the mass loss steps and the mechanism for the mass loss to be determined [21–27]. Thermoanalytical methods can provide a measure of the thermal stability of the clay minerals [21–46]. Controlled rate thermal analysis (CRTA) has proven extremely worthwhile in the study of the stability and thermal decomposition pathways of minerals and modified minerals such as mechanochemically activated kaolinite and intercalated kaolinites [26, 35, 47–52]. The application of CRTA technology to the study of the thermal stability of sepiolites has to the best of our knowledge never been reported. In this work we report the thermal analysis using both dynamic and controlled rate thermal analysis (CRTA technology) of sepiolite.

Experimental

Minerals

The clay minerals used in this research are (a) Clay Mineral Repository standard sepiolite from Nevada [SepNev-1] (b) sepiolite from Nairobi. Further details of these source clays can be found at the web site [<http://cms.lnl.gov>]. The chemical composition of the sepiolite from Nevada is in %: SiO₂: 54.0, Al₂O₃: 0.5, TiO₂: <.001, Fe₂O₃: 0.81, FeO: <0.1, MnO: 0.11, MgO: 23.3, CaO: 1.25, Na₂O: 2.1, K₂O: 0.15, P₂O₅: 0.02, LOI: 19.2. The chemical composition of the sepiolite from Nairobi in % is: SiO₂: 52.9, Al₂O₃: 2.56, TiO₂: <.001, Fe₂O₃: 1.22, FeO: 0.3, MnO: 0.13, MgO: 23.6, CaO: <.01, Na₂O: <0.01, K₂O: 0.05, P₂O₅: 0.01, LOI: 20.8. The two sepiolites are reasonably close to the theoretical formula Mg₈Si₁₂O₃₀(OH)₄·(H₂O)₄·8H₂O. The clays were analysed by X-ray diffraction for phase purity and dried in a

desiccator to remove adsorbed water before being submitted for thermal analysis. The clay minerals were ground to a fine powder of <0.5 μm particle size for thermal analysis.

Thermal analysis

Dynamic experiment

Thermal decomposition of the sepiolite was carried out in a Derivatograph PC type thermoanalytical equipment (Hungarian Optical Works, Budapest, Hungary) capable of recording the thermogravimetric (TG), derivative thermogravimetric (DTG) and differential thermal analysis (DTA) curves simultaneously. The sample was heated in a ceramic crucible in static air atmosphere at a rate of 5 °C min⁻¹.

Controlled rate thermal analysis experiment

Thermal decomposition of the sepiolites was carried out in a Derivatograph PC-type thermoanalytical instrument in a flowing air atmosphere (250 cm³/min) at a pre-set, constant decomposition rate of 0.10 mg min⁻¹ (below this threshold value the samples were heated under dynamic conditions at a uniform rate of 0.10 °C min⁻¹). The samples were heated in an open ceramic crucible at a rate of 0.10 °C min⁻¹ up to 300 °C. With the quasi-isothermal, quasi-isobaric heating program of the instrument the furnace temperature was regulated precisely to provide a uniform rate of decomposition in the main decomposition stage.

Results and discussion

Dynamic thermal analysis of sepiolite

The dynamic thermal analysis results for a sepiolite from Nevada and Nairobi are shown in Figs. 1 and 2. The figures

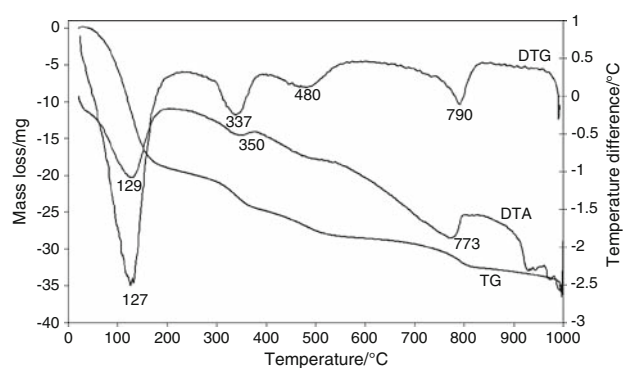


Fig. 1 The dynamic thermogravimetric and differential thermogravimetric analysis of sepiolite from Nevada—clay mineral reference standard SEPND-1

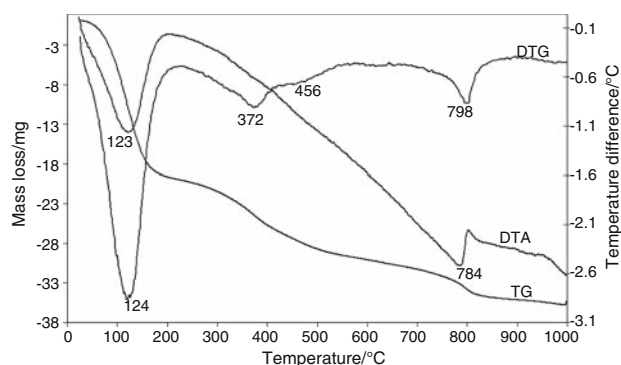
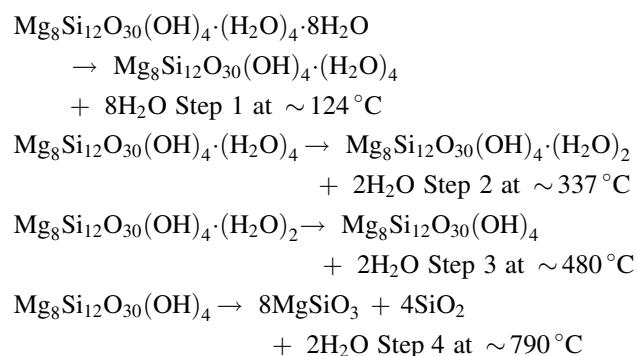


Fig. 2 The dynamic thermogravimetric and differential thermogravimetric analysis of sepiolite from Nairobi

report the DTG, DTA and TG curves. Four distinct mass losses are observed in the thermogravimetric and differential thermogravimetric curves in Fig. 1 at 127, 337, 480 and 790 °C with % mass losses of 12.4, 3.2, 2.5, 2.7 and 1.6%. In the DTA curve endotherms are observed at 129, 350, 480 and 773 °C. The results are similar for the thermal analysis of the sepiolite from Nairobi (Fig. 2). Peaks in the DTG curves occur at 124, 372, 456 and 798 °C. The % mass losses are 10.9, 3.5, 1.8, 2.9 and 0.4%. The endotherms for the DTA pattern for this sepiolite are not as distinct with endotherms observed at 123, 370, 460 and 798 °C.

Nagata et al. proposed a set of steps for the dehydration and dehydroxylation of a sepiolite [16, 53]. These steps correspond to (a) the loss of adsorbed water (b) the loss of hydration water (c) the loss of coordination water (d) the loss of water through dehydroxylation. Such a scheme is represented by the following chemical equations:



Such a scheme is an apparent oversimplification as each of these steps may be subdivided into component mass loss steps. If one uses the formula $(\text{Mg}_8\text{Si}_{12}\text{O}_{30}(\text{OH})_4 \cdot (\text{H}_2\text{O})_4 \cdot 8\text{H}_2\text{O})$ for sepiolite then the theoretical mass loss for step 1 should be 11.0%. The % mass loss observed for the DTG curve for sepiolite from Nevada was 12.4%. The theoretical mass loss for step 2 is 2.76% compared with the observed value of 3.2% which is in excellent agreement with the theoretical value. The third step theoretical mass

loss also should be 2.76% and a value of 2.5% is observed. The final mass loss step should be 5.21%; 4.3% mass loss is found. Thus there is excellent agreement with the predicted and the observed mass loss values. The observation that the experimentally determined mass loss step is less than that predicted is an indication that some dehydroxylation may have taken place in the previous steps with the evolution of the bound water. It has been found that sepiolite folds to the anhydride like form when about half the H_2O of coordination is removed, at $<200^\circ\text{C}$ in vacuum or at approximately 300°C in air [18–20]. Removal of the remaining H_2O at 530°C under reduced pressure produces little further structural change. Infrared evidence suggests that partially dehydrated sepiolite is a folded structure with H_2O of coordination trapped in hexagonal holes. The remaining H_2O is lost, without significant structural change, at $\sim 500^\circ\text{C}$ under vacuum to give a true anhydride [21–24]. A previous thermo-analytical study by the author found similar results for a wide range of sepiolites and palygorskites [51].

Controlled rate thermal analysis of sepiolite

The controlled rate thermal analysis of the sepiolites from Nevada and Nairobi are shown in Figs. 3 and 4. The results

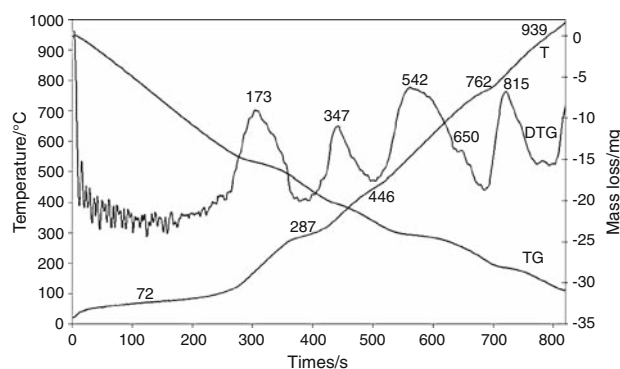


Fig. 3 The controlled rate thermal analysis of sepiolite from Nevada

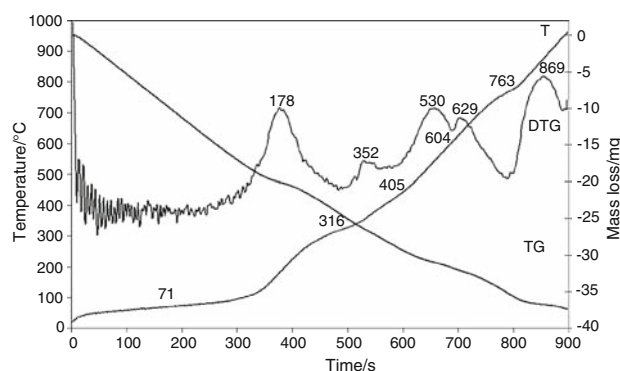


Fig. 4 The controlled rate thermal analysis of sepiolite from Nairobi

Table 1 Decomposition stages of sepiolites under CRTA conditions

Decomposition process	Sepiolite, Nevada (sample mass: 152.31 mg)			Sepiolite, Nairobi (sample mass: 196.89 mg)		
	Temp. range/°C	Mass loss		Temp. range/°C	Mass loss	
		mg	%		mg	%
Dehydration	22–171	15.3	10.0	22–178	20.1	10.2
	171–347	5.0	3.3	178–352	6.3	3.2
Dehydroxylation	347–542	3.8	2.5	352–530	4.5	2.3
	542–815	4.0	2.6	530–627	1.2	0.6
	815–989	2.8	1.8	627–871	4.7	2.4
					871–957	0.6

of the thermal analysis are reported in Table 1. The first two steps are assigned to the dehydration of the sepiolite and the next three steps to dehydroxylation of the clay. In the CRTA experiment water is lost in a quasi isothermal step at 72 °C followed by a non-isothermal step at 287 °C. In the first step 10.0% of the total mass is lost and 3.3% in the second step. If one uses the formula $(Mg_8Si_{12}O_{30}(OH)_4 \cdot (H_2O)_4 \cdot 8H_2O)$ for sepiolite then the theoretical mass loss for step 1 should be 11.0%. The % mass loss observed for the CRTA curve for sepiolite from Nevada was 10.0%. The theoretical mass loss for step 2 is 2.76% compared with the observed value of 3.3% which is in excellent agreement with the theoretical value. For the Nairobi sepiolite a similar set of results is obtained. For the dehydroxylation mass losses of 10.2 and 3.2% are observed. For the sepiolite from Spain, mass losses of 7.3 and 4.1% were found (Fig. 5).

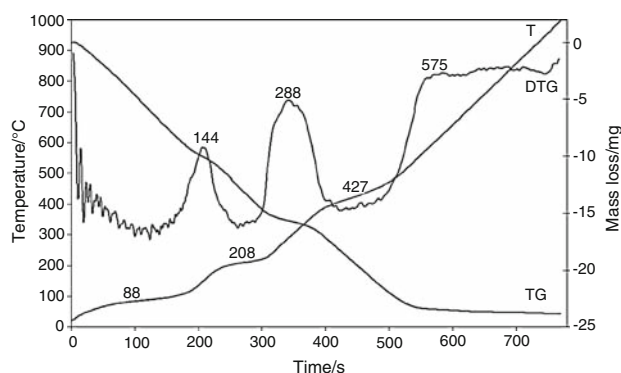
The OH units appear to be lost in three or four non-isothermal steps at 446, 762 and 939 °C. In the first three steps for the Nevada sepiolite over the 347–542, 542–815 and 815–939 temperature ranges, 2.5, 2.6 and 1.8% mass losses are found. Using the formula $(Mg_8Si_{12}O_{30}(OH)_4 \cdot (H_2O)_4 \cdot 8H_2O)$ for sepiolite, the theoretical mass loss for first dehydroxylation step is 2.76% compared with the observed value of 2.5% which is in excellent agreement with the theoretical value. The second dehydroxylation

step, theoretical mass loss also should be 2.76% and a value of 2.6% is observed. The third mass loss step should be 5.21%. However, only 1.8% mass loss is found. In Fig. 3 an additional dehydroxylation step at 650 is observed. For the sepiolite from Nairobi in the CRTA experiment, four dehydroxylation steps are observed over the 352–530, 530–627, 627–871, 871–957 temperature range with mass losses of 2.3%, 0.6%, 2.4% and 0.3%.

Conclusions

The number of steps in the thermal analysis of sepiolites are greater compared with previous published results when using dynamic high resolution DTG and CRTA techniques. The CRTA experiment enables the separation of mass losses for the dehydration steps of sepiolite minerals. Two dehydration steps for sepiolite are observed. These occur around 70–90 °C, and 210–320 °C. Three dehydroxylation steps for sepiolite are observed in the CRTA experiment. A low temperature mass loss at 350–400 °C and a higher temperature mass loss above 500 °C. Significant differences in the results as determined by the dynamic and CRTA experiment are observed.

CRTA technology offers better resolution and a more detailed interpretation of the decomposition processes of a clay mineral such as sepiolite via approaching equilibrium conditions of decomposition through the elimination of the slow transfer of heat to the sample as a controlling parameter on the process of decomposition. Constant-rate decomposition processes of non-isothermal nature reveal partial collapse of the layers of sepiolite as the sepiolite is converted to an anhydride, since in this cases a higher energy (higher temperature) is needed to drive out gaseous decomposition products through a decreasing space at a constant, pre-set rate. The CRTA experiment proves the thermal decomposition of sepiolites from different sources are almost identical. The CRTA technology offers a mechanism for the study of the thermal decomposition of minerals such as sepiolite.

**Fig. 5** The controlled rate thermal analysis of sepiolite from Spain

Acknowledgements This research was supported by the Hungarian Scientific Research Fund (OTKA) under Grant No. K62175. The financial and infra-structure support of the Queensland University of Technology Inorganic Materials Research Program is gratefully acknowledged. One of the authors (LMD) is grateful to the CRC for polymers for a Masters scholarship.

Appendix

Calculation of water content for Sepiolite, Nevada:

Composition: $\text{Mg}_4\text{Si}_6\text{O}_{15}(\text{OH})_2 \cdot x\text{H}_2\text{O}$

Removing water up to 347 °C: 20.30 mg that is 1.127 mmol

Remaining dehydrated mineral up to 347 °C: 132.01 mg that is 0.245 mmol

Molar mass of dehydrated mineral: 539.80 g/mol

Calculation of x :

1 mol dehydrated mineral – x mol H_2O

0.245 mol dehydrated mineral – 1.127 mol H_2O

$x = 4.6\text{--}5$ mol

Formula: $\text{Mg}_4\text{Si}_6\text{O}_{15}(\text{OH})_2 \cdot 5\text{H}_2\text{O}$

Steps of water liberation according to the decomposition steps up to 347 °C:

1. step: 3.45 mol
2. step: 1.15 mol

Calculation of water content for Sepiolite, Nairobi:

Composition: $\text{Mg}_4\text{Si}_6\text{O}_{15}(\text{OH})_2 \cdot x\text{H}_2\text{O}$

Removing water up to 352 °C: 26.40 mg that is 1.465 mmol

Remaining dehydrated mineral up to 352 °C: 170.49 mg that is 0.316 mmol

Molar mass of dehydrated mineral: 539.80 g/mol

Calculation of x :

1 mol dehydrated mineral – x mol H_2O

0.316 mol dehydrated mineral – 1.465 mol H_2O

$x = 4.63\text{--}5$ mol

Formula: $\text{Mg}_4\text{Si}_6\text{O}_{15}(\text{OH})_2 \cdot 5\text{H}_2\text{O}$

Steps of water liberation according to the decomposition steps up to 352 °C:

1. step: 3.53 mol
2. step: 1.10 mol

References

1. Caillere S, Henin S. The application of differential thermal analysis to the study of the clay minerals found in soils. *Ann Agron.* 1947;17:23–72.
2. Sudo T, Hayashi H. New types of clay minerals with long spacings at about 30 Å. found from the altered area developed around certain ore bodies of the Hanaoka Mine, Akita Prefecture. Science reports. Tokyo Kyoiku Daigaku C Geol Miner Geogr. 1955;3:281–94.
3. Koltermann M, Rauschenfels E, Pfefferkorn H. The thermal behavior of sepiolite. *Tonind-Ztg Keram Rundschau.* 1964;88:132–4.
4. Murat M, Gielly J. Reactions of dehydration and dehydroxylation of clay minerals studied by electric conductivity measurements and differential thermal analysis. *Bull Groupe Fr Argiles.* 1969;21:151–76.
5. Hayashi H, Otsuka R, Imai N. Infrared study of sepiolite and palygorskite on heating. *Am Miner.* 1969;54:1613–24.
6. Vicente MA, Suarez M, Lopez-Gonzalez JD, Banares-Munoz MA. Characterization, surface area, and porosity analysis of the solids obtained by acid leaching of a saponite. *Langmuir.* 1996;12:566–72.
7. Kinoshita R, Ichimura Y, Onodera J, Niimura N, Nakayama Y, Higuchi T. The optimization of the TG/DTA-MS measurements and the application for the material analysis. *J Mass Spectrom Soc Jpn.* 1998;46:365–73.
8. Brigatti MF, Franchini GC, Medici L, Poppi L, Stewart A. Behavior of sepiolite in Co^{2+} , Cu^{2+} and Cd^{2+} removal from a simulated pollutant solution. *Ann Chim (Rome).* 1998;88:461–70.
9. Yariv S, Lapidés I. The effect of mechanochemical treatments on clay minerals and the mechanochemical adsorption of organic materials onto clay minerals. *J Mater Synth Process.* 2000;8:223–33.
10. Cebulak S, Langier-Kuzniarowa A. Some remarks on the methodology of thermal analysis of clay minerals. *J Therm Anal Calorim.* 1998;53:375–81.
11. Perez-Rodriguez JL, Galan E. Determination of impurity in sepiolite by thermal analysis. *J Therm Anal Calorim.* 1994;42:131–41.
12. Aramendia MA, Borau V, Corredor JI, Jimenez C, Marinas JM, Ruiz JR, et al. Characterization of the structure and catalytic activity of Pt/sepiolite catalysts. *J Colloid Interface Sci.* 2000;227:469–75.
13. Fernandez Alvarez T. Studies of pore structure of various solids by nitrogen adsorption. I. Natural sepiolites activated by hydrochloric acid. In: *Proc int clay conf.* 1973. p. 571–82.
14. Serna C, Ahlrichs JL, Serratos JM. Folding in sepiolite crystals. *Clays Clay Miner.* 1975;23:452–7.
15. Serna C, Rautureau M, Prost R, Tchoubar C, Serratos JM. Study of sepiolite with the aid of data from electronic microscopy, thermogravimetric analysis, and infrared spectroscopy. *Bulletin du Groupe Francais des Argiles.* 1974;26:153–63.
16. Nagata H, Sudo T. Dehydration and dehydroxylation of sepiolite. In: *Therm. anal., [proc. int. conf.], 5th.* 1977. p. 534–7.
17. Yariv S. Combined DTA-mass spectrometry of organo-clay complexes. *J Therm Anal Calorim.* 1990;36:1953–61.
18. Serna C, Ahlrichs JL, Serratos JM. Sepiolite anhydride and crystal folding. *Clays Clay Miner.* 1975;23:411–2.
19. Serna C, VanScoyoc GE, Ahlrichs JL. Hydroxyl groups and water in palygorskite. *Am Mineral.* 1977;62:784–92.
20. Serna C, VanScoyoc GE, Ahlrichs JL. Uncoupled water found in palygorskite. *J Chem Phys.* 1976;65:3389–90.
21. Frost RL, Erickson KL. Thermal decomposition of synthetic hydrotalcites reevesite and pyroaurite. *J Therm Anal Calorim.* 2004;76:217–25.
22. Horvath E, Kristof J, Frost RL, Heider N, Vagvolgyi V. Investigation of $\text{IrO}_2/\text{SnO}_2$ thin film evolution by thermoanalytical and spectroscopic methods. *J Therm Anal Calorim.* 2004;78:687–95.
23. Frost RL, Weier ML, Erickson KL. Thermal decomposition of struvite. *J Therm Anal Calorim.* 2004;76:1025–33.
24. Frost RL, Erickson KL. Thermal decomposition of natural iowaite. *J Therm Anal Calorim.* 2004;78:367–73.
25. Horvath E, Kristof J, Frost RL, Redey A, Vagvolgyi V, Cseh T. Hydrazine-hydrate intercalated halloysite under controlled-rate thermal analysis conditions. *J Therm Anal Calorim.* 2003;71:707–14.

26. Kristof J, Frost RL, Klopogge JT, Horvath E, Mako E. Detection of four different OH-groups in ground kaolinite with controlled-rate thermal analysis. *J Therm Anal Calorim.* 2002;69:77–83.
27. Frost RL, Martens W, Ding Z, Klopogge JT. DSC and high-resolution TG of synthesized hydrotalcites of Mg and Zn. *J Therm Anal Calorim.* 2003;71:429–38.
28. Bouzaid J, Frost RL. Thermal decomposition of stichtite. *J Therm Anal Calorim.* 2007;89:133–5.
29. Bouzaid JM, Frost RL, Martens WN. Thermal decomposition of the composite hydrotalcites of iowaite and woodallite. *J Therm Anal Calorim.* 2007;89:511–9.
30. Bouzaid JM, Frost RL, Musumeci AW, Martens WN. Thermal decomposition of the synthetic hydrotalcite woodallite. *J Therm Anal Calorim.* 2006;86:745–9.
31. Frost RL, Bouzaid JM, Musumeci AW, Klopogge JT, Martens WN. Thermal decomposition of the synthetic hydrotalcite iowaite. *J Therm Anal Calorim.* 2006;86:437–41.
32. Frost RL, Ding Z, Ruan HD. Thermal analysis of goethite. Relevance to Australian indigenous art. *J Therm Anal Calorim.* 2003;71:783–97.
33. Frost RL, Erickson K, Weier M. Thermal treatment of moolooite. *J Therm Anal Calorim.* 2004;77:851–61.
34. Frost RL, Kristof J, Martens WN, Weier ML, Horvath E. Thermal decomposition of sabugalite. *J Therm Anal Calorim.* 2006;83:675–9.
35. Frost RL, Kristof J, Weier ML, Martens WN, Horvath E. Thermal decomposition of metatorbernite—a controlled rate thermal analysis study. *J Therm Anal Calorim.* 2005;79:721–5.
36. Frost RL, Martens W, Adebajo MO. Synthesis of the mixed oxide catalysts based upon the nickel-copper hydrotalcites of the type $\text{Ni}_x\text{Cu}_{6-x}\text{Cr}_2(\text{OH})_{16}(\text{CO}_3)_4\text{H}_2\text{O}$. *J Therm Anal Calorim.* 2005;81:351–5.
37. Frost RL, Musumeci AW, Adebajo MO, Martens W. Using thermally activated hydrotalcite for the uptake of phosphate from aqueous media. *J Therm Anal Calorim.* 2007;89:95–9.
38. Frost RL, Musumeci AW, Klopogge JT, Weier ML, Adebajo MO, Martens W. Thermal decomposition of hydrotalcite with hexacyanoferrate(II) and hexacyanoferrate(III) anions in the interlayer. *J Therm Anal Calorim.* 2006;86:205–9.
39. Frost RL, Weier ML. Thermal decomposition of humboldtine—a high resolution thermogravimetric and hot stage Raman spectroscopic study. *J Therm Anal Calorim.* 2004;75:277–91.
40. Frost RL, Weier ML, Martens W. Thermal decomposition of jarosites of potassium, sodium and lead. *J Therm Anal Calorim.* 2005;82:115–8.
41. Frost RL, Weier ML, Martens W. Thermal decomposition of liebigite: a high resolution thermogravimetric and hot-stage Raman spectroscopic study. *J Therm Anal Calorim.* 2005;82:373–81.
42. Frost RL, Wills R-A, Klopogge JT, Martens W. Thermal decomposition of ammonium jarosite $(\text{NH}_4)\text{Fe}_3(\text{SO}_4)_2(\text{OH})_6$. *J Therm Anal Calorim.* 2006;84:489–96.
43. Frost RL, Wills R-A, Klopogge JT, Martens WN. Thermal decomposition of hydronium jarosite $(\text{H}_3\text{O})\text{Fe}_3(\text{SO}_4)_2(\text{OH})_6$. *J Therm Anal Calorim.* 2006;83:213–8.
44. Lin Y-H, Adebajo MO, Frost RL, Klopogge JT. Thermogravimetric analysis of hydrotalcites based on the takovite formula $\text{Ni}_x\text{Zn}_{6-x}\text{Al}_2(\text{OH})_{16}(\text{CO}_3)_4\text{H}_2\text{O}$. *J Therm Anal Calorim.* 2005;81:83–9.
45. Musumeci AW, Silva GG, Martens WN, Waclawik ER, Frost RL. Thermal decomposition and electron microscopy studies of single-walled carbon nanotubes. *J Therm Anal Calorim.* 2007;88:885–91.
46. Xi Y, Martens W, He H, Frost RL. Thermogravimetric analysis of organoclays intercalated with the surfactant octadecyltrimethylammonium bromide. *J Therm Anal Calorim.* 2005;81:91–7.
47. Frost RL, Kristof J, Horvath E, Klopogge JT. The modification of hydroxyl surfaces of formamide-intercalated kaolinites synthesized by controlled rate thermal analysis. *J Colloid Interface Sci.* 2001;239:126–33.
48. Frost RL, Kristof J, Horvath E, Klopogge JT. Separation of adsorbed formamide and intercalated formamide using controlled rate thermal analysis methodology. *Langmuir.* 2001;17:3216–22.
49. Frost RL, Kristof J, Horvath E, Martens WN, Klopogge JT. Complexity of intercalation of hydrazine into kaolinite—a controlled rate thermal analysis and DRIFT spectroscopic study. *J Colloid Interface Sci.* 2002;251:350–9.
50. Ding Z, Frost RL. Controlled rate thermal analysis of nontronite. *Thermochim Acta.* 2002;389:185–93.
51. Frost RL, Ding Z. Controlled rate thermal analysis and differential scanning calorimetry of sepiolites and palygorskites. *Thermochim Acta.* 2003;397:119–28.
52. Frost RL, Kristof J, Ding Z, Horvath E. Controlled rate thermal analysis of formamide intercalated kaolinites, 2001 a clay odyssey. In: *Proceedings of the international clay conference, 12th, Bahia Blanca, Argentina, July 22–28, 2001.* 2003. p. 523–30.
53. Nagata H. Thermal analysis of sepiolite by means of DSC. *Nendo Kagaku.* 1977;17:1–11.